Novel germline RB1 and MET gene mutations in a case with bilateral retinoblastoma followed by multiple metastatic osteosarcoma

Attila Mokánszki[1], Chang Yi-Che[1], János Mótyán[1], Péter Juhász[1], Emese Bádon[1], László Madar[1], István Szegedi[1], Csongor Kiss[2], and Gábor Méhes[1]

[1]University of Debrecen Faculty of Medicine
[2]University of Debrecen

November 11, 2020

Abstract

Background Retinoblastoma (Rb) is a malignant tumor of the developing retina that affects children before the age of five years in association with inherited or early germline mutations of the RB1 gene. The genetic predisposition is also related with second primary malignancies arising de novo, or following radiotherapy which have become the leading cause of death in retinoblastoma survivors. Procedure We describe a retinoblastoma case with a novel RB1 and a synchronous MET aberration. Our goal was to identify all germline and somatic genetic alterations in available tissue samples from different time periods and to reconstruct their clonal relations using next generation sequencing (NGS). We also used structural and functional prediction of the mutant RB and MET proteins to find interactions between the defected proteins with potential causative role in the development of this uniqe form of retinoblastoma. Results In this study we detected a retinoblastoma case of non-parental origin with a novel RB1 c.2548C>T;p.(Gln850Ter) and a synchronous MET c.3029C>T;p.(Thr1010Ile) germline mutations. Following bilateral retinoblastoma the boy further developed at least four different manifestations of two independent osteosarcomas. Both histopathology and NGS findings supported the independent nature of a chondroblastic osteosarcoma of the irradiated facial bone followed by an osteoblastic sarcoma of the leg (tibia). Conclusions Because of the expanding number of registered Rb cases, the novel rare cases publication is very important to understand the molecular mechanism of this malignancy. We reported a novel form of Rb and consequential chondroblastic and osteoblastic osteosarcoma, the latter one developing pulmonary metastatses.

Introduction

Retinoblastoma (Rb, OMIM#180200) is a malignant tumor of the developing retina that affects children before the age of five years with an estimated incidence between 1 in 16,000 and 1 in 18,000 live births [1]. Rb occurs in both heritable (25-30%) and non-heritable (70-75%) forms. A heritable form is defined by the presence of a germline heterozygotic mutation in the *RB1* gene (Genbank accession number L11910.1; NCBI RefSeq NM_000321.2), wich is followed by a second somatic hit in the developing retina. As a result, tumors affecting either one (unilateral) or both (bilateral) eyes may develop. In the non-heritable form both mutations occur in somatic cells, usually leading to unilateral malignancy [2]. In addition to the highly malignant early onset Rb, the risk of developing second cancers, e.g. osteosarcomas and other soft-tissue sarcomas, rarely melanomas is increased. Molecular diagnostics is required to clear heredity status and to deliver the best options for the management of the disease [3, 4]. Due to the genetic predisposition, second primary malignancies may arise spontaneously or following radiotherapy, which have become the leading cause of death in Rb survivors. Osteosarcomas in retinoblastoma patients occurred 1.2 years earlier and the latency period between radiotherapy and osteosarcoma onset was 1.3 years shorter inside than outside of the

1

radiation field [5].

The *RB1* gene shows a wide spectrum of mutations, including single nucleotide variants (SNVs), small insertions/deletions (indels), and large deletions/duplications. These mutations are distributed throughout the entire length of the gene, spanning over 27 exons, and no hotspots have been reported [6]. New advances in molecular genetic testing, and especially next-generation sequencing (NGS), allow the comprehensive demonstration of all SNVs and large aberrations throughout the full length of the gene. Pathogenic mutations in both alleles of the*RB1* gene are related to the development of this neoplasm in the large majority of the cases. Alternatively, complex mutation patterns missing the *RB1* gene aberration were identified in rare cases of manifest Rb, indicating to oncogenic interactions between different signal transduction pathways [7].

The aim of our study was (i) to identify germline genetic aberrations in a patient with bilateral Rb of non-parental origin, (ii) to exclude the parental carrier status, (iii) to characterize histological and genetic features of samples originating from the two Rb and the four anatomically distinct osteosarcoma tumors (iv) to genetically differentiate between the irradiation-related orbitofacial and the non-related *de novo* osteosarcoma of the lower extremity, (v) structural and functional prediction of the germline mutant proteins reconstructed after DNA sequencing, and, finally (vi) identify potential interaction between defected proteins using prediction analysis. For this purpose, histology, including immunohistochemistry (IHC) and NGS solid tumor gene panel (Illumina MiSeq platform) analysis were performed using samples from both enucleated eyes and from the four available osteosarcoma tissues. Autopsy sample of the skin was taken as normal non-neoplastic control tissue. In addition, *in silico* prediction methods were applied to analyse the secondary structure and functionality of detected germline variants and to predict protein-protein interaction. To exclude potential parental origin conventional Sanger sequencing was used.

Materials and Methods

Patients samples

Altogether seven formaldehyde-fixed paraffin-embedded tissue (FFPE) samples were tested from the patient diagnosed with Rb/osteosarcoma in 2010 and followed until his death in 2019 at the Department of Pediatrics, University of Debrecen (**Table 1.**). Peripheral blood samples from both parents was collected for analysing their carrier status. Sampling was agreed and supported by a written consent from both sides. All protocols have been approved by the author's respective Institutional Review Board for human subjects (IRB reference number: 60355/2016/EKU) and conducted in accorcance with the Helsinki Declaration.

Histology and immunohistochemistry

Hematoxylin and eosin (H&E) stained slides were carefully analysed and validated by pathology specialists and appropriate tumor samples were selected for DNA isolation with a tumor percentage >20% (in samples where lower tumor ratio was detected, microdissection was performed). IHC of neuron specific enolase (NSE, BBS/NC/VI-H14 clone, 1:800 dilution, Agilent Technologies, Santa Clara, CA, USA) and synaptophysin (27G12 clone, 1:100 dilution, Leica Biosystems, Wetzlar, Germany) was performed to confirm Rb diagnosis. Anti-RB monoclonal antibody (1F8 (RB1) clone, 1:200 dilution, Invitrogen, Carlsbad, CA, USA) was used on all samples of the patient and on a control colorectal adenocarcinoma sample.

DNA isolation

DNA isolation from peripherial blood was performed using QIAamp DNA Mini Kit (Qiagen, Hilden, Germany). Genomic DNA was extracted from FFPE tissues using the QIAamp DNA FFPE Tissue Kit (Qiagen, Hilden, Germany). The isolations were carried out according to the manufacturer's standard protocol and the DNA was eluted in 50 μL elution buffer. The DNA concentration was measured in the Qubit dsDNA HS Assay Kit using a Qubit 4.0 Fluorometer (Thermo Fisher Scientific, Waltham, MA, USA).

Sanger sequencing

RB1 mutation testing, with special attention toward exon 25, was performed using conventional Sanger sequencing on all DNA samples originating from FFPE blocks of the patient and on the peripherial blood

2

DNA samples of their parents. The purified PCR products were sequenced using both forward and reverse primers (which were used for the PCR amplification) using the BigDye Terminator v3.1 Cycle Sequencing kit. The samples were analysed on the ABI PRISM 310 Genetic Analyzer (Thermo Fisher Scientific, Waltham, MA, USA).

Next-Generation sequencing

The amount of amplifiable DNA (ng) was calculated according to the Archer PreSeq DNA Calculator Assay Protocol (Archer DX, Boulder, CO, USA). After fragmentation of the genomic DNA, libraries were created by the Archer VariantPlex Solid Tumor Kit (Archer DX, Boulder, CO, USA). The KAPA Universal Library Quantification Kit (Kapa Biosystems, Roche, Basel, Switzerland) was used for the final quantification of the libraries.

The MiSeq System (MiSeq Reagent kit v3 600 cycles, Illumina, San Diego, CA, USA) was used for sequencing. The libraries (final concentration of 4 nM, pooled by equal molarity) were denatured by adding 0.2 nM NaOH and diluted to 40 pM with hybridization buffer from Illumina (San Diego, CA, USA). The final loading concentration was 8 pM libraries and 1% PhiX. Sequencing was conducted according to the MiSeq instruction manual. Captured libraries were sequenced in a multiplexed fashion with paired end run to obtain 2x150 bp reads with at least 250X depth of coverage. The trimmed fastq files were generated using MiSeq reporter (Illumina, San Diego, CA, USA).

Raw sequence data were analysed with Archer analysis software (version 6.2.; Archer DX, Boulder, CO, USA) for the presence of single-nucleotide variants (SNVs) as well as insertions and deletions (indels). For the alignment, the human reference genome GRCh37 (equivalent UCSC version hg19) was built. Molecular barcode (MBC) adapters were used to count unique molecules and characterized sequencer noise, revealing mutations below standard NGS-based detection thresholds. The sequence quality for each sample was assessed and the cutoff was set to 5% variant allele fraction. Large insertion/deletion (>50 bp) and complex structural changes could not be captured by the method. The results were described using the latest version of Human Genome Variation Society nomenclature for either the nucleotide or protein level. Individual gene variants were cross-checked in the COSMIC (Catalogue of Somatic Mutations in Cancer) and ClinVar databases for clinical relevance.We used gnomAD v.2.1.1 population database to compare the significance of each gene alterations which is included in our Archer NGS analysis system.

Protein in silico methods

Protein information for RB protein (P06400, RB_HUMAN) and for hepatocyte growth factor receptor MET (P08581, MET_HUMAN) were obtained from UniProt database and from RCSB Protein Data Bank. GOR method version IV was used for secondary structure prediction [8]. Disorder prediction was performed by IUPred2A web server [9]. Eukaryotic linear motifs (ELM) were identified in the proteins by using ELM database [10]. Stability changes upon point mutations were predicted by I-Mutant 2.0 web server based on protein sequence, using default parameters [11]. Protein-protein interaction data were obtained from BioGRID [12] and STRING databases [13].

Results

Clinical presentation and therapeutic actions

A one year-old boy with Rb suspicion was referred to the Department of Pediatrics, University of Debrecen. Given the bilateral, large primary extent of the tumor not suitable for local therapy systemic chemotherapy was immediately introduced. Two cyclophosphamide/vincristine block, advised for infant neuroblastoma was applied with partial response. Thus therapy was continued with three more intensive carboplatin/etoposide/vincristine block, but without further tumor regression, so three additional VEC (vincristine/etoposide/cyclophosphamide) was introduced that resulted in significant tumor regression making possible local therapy. Until the local intervention two additional VEC was applied with decreased (60%) dose in view of the patient tolerance. Then a local brachytherapy (Ruthenium-106 applicator) was applied on the right side, and cryotherapy on the left side. Five months later a progression was observed on the right

3

side that extend the local control borders. As a bridge therapy VEC with cisplatin, then 50 Gy external radiotherapy was applied for both sides. However, progression was occured five months later, so enucleation was necessary on the right, and then unfortunately on the left side three months apart (Sample 1 – S1 and 2 - S2). Telemetric radiotherapy followed enucleation on both sides in 50 Gy doses. The proband, at the age of 10 years presented osteosarcoma of the left orbita that was surgically resected (S3). EURAMOS1 and than EURO EWING99-VIDE protocol was used for chemotherapy. One year later osteosarcoma presented on the left tibia as well and was resected 17 cm of the its proximal region (S4). Resected tibial bone was irradiated using 100 Gy and EURAMOS1/COSS chemotherapy was applied. At the age of 12 years, left femur and multiple pulmonary metastases were diagnosed. Up to the upper third, the left femur was amputated and osteosarcoma was proved by histological examination (S5). According to the bad general condition of the child, pulmonary tumor was sentenced as inoperable. Three months later the proband died due to breathing complications. Progressive metastases of both sides of the lungs were demonstrated as cause of death during autopsy. Postmortem sampling from the pulmonary metastases (S6) and from the intact skin (sample S7, for non-tumor control purposes) was done. Samples provided for the comparative study and related histological diagnoses are summarized in **Table 1** .

Histological examination

Sections from the left and right ocular tumors showed a picture of small round cell tumor with high mitotic activity and tumor necrosis. The tumor cells possessed neuroendocrine immunophenotype (NSE and synaptophysin positivity). Diagnosis of Rb was established.

The sections from the left orbital and left tibia/femoral tumors revealed chondroblastic and osteoblastic osteosarcoma, respectively, with high grade, bizarre tumor cells proliferation and osteioid production. The former sample also showed excess amount of malignant cartilaginous component. The lung tumour showed classical osteoblastic osteosarcoma indicating the metastatic nature from the lower leg. Key histological features are shown in **Figure 1** .

Germline gene mutations

In all samples of the patient the same c.2548C>T; p.(Gln850Ter) mutation of the *RB1* gene were detected in a heterozygotic form (variant allele frequence (VAF): 50±10%). In addition, the c.3029C>T; p.(Thr1010Ile)/c.2975C>T; p.(Thr992Ile) variant of the*MET* gene was identified throughout the samples (VAF range: 27 to 50%). Targeted Sanger sequencing of the parental DNA isolated from the peripheral blood did not detect the mutations in question.

Immunohistochemistry of the RB protein

The detected germline *RB1* gene mutation suggested the generation of a truncated RB protein following translation. The histological localisation and intracellular distribution of the aberrant protein was analysed using an anti-RB monoclonal antibody on all samples and on known positive controls (colorectal adenocarcinoma). While the nuclear localisation of the RB protein was shown in control slides it was not detected in the patient samples. RB IHC of the S1, the S3 and the control was presented in **Figure 2** .

Somatic gene mutations

The molecular genetic results of the samples originating from the different tumor type are presented in **Table 2** .

In the right bulbus Rb sample (S1) *CTNNB1* and *EZH2*mutations were identified opposite to the S2 (left bulbus) tumor, where*ALK* , *APC* and *CDH1* variants were detected.*EZH2* aberration emerged in the all tumor samples, but not in the non-tumor control, therefore, this was considered as a tumor-specific somatic gene variant. In the chondroblastic osteosarcoma sample (S3) no other somatic mutations were detected. In contrast, all osteoblastic osteosarcoma samples (S4-S6) featured the same *TP53* pathogenic variant with high VAF (38.4-69.0%). Additional variants of the genes*ERBB* , *HRAS* and *SMAD4* were identified at the level of the individual samples.

4

In silico analysis of RB and hepatocyte growth factor receptor (MET) mutant proteins

The p.(Gln850Ter) mutation of RB protein causes a truncation of the full-length protein (1-928) by 78 residues (**Figure 3**). The deletion of the C-terminal region (851-928 residues) was predicted to cause no alteration of the secondary structural arrangement, neither local nor long-distance effect were predicted for the truncated protein. Disorder prediction also showed that the truncation of the protein does not cause significant changes in pathogenicity.

Neither secondary structure nor disorder predictions showed any adverse effects of the deletion on protein structure. Therefore, the consequence of the truncation can be associated with the loss of functional regions. The functional importance of the C-terminal region in RB protein is implied by the presence of ELMs, including a bipartite nuclear localization signal (860-876). Consequently, the loss of this signal sequence may result an impaired nuclear localization of the mutant/truncated protein, while the wild-type protein naturally enters the nucleus. The structure and possible interactions of RB1 protein was presented in **Figure 3** . The following coordinate files were used to prepare the figure: 2QDJ.pdb [14]; 4ELL.pdb [15]; 2AZE.pdb [16]; 3N5U.pdb [17]; 1H25.pdb [18]; 1PJM [19].

The p.(Thr1010Ile) mutation of MET protein causes a non-synonymous mutation of a polar threonine to a hydrophobic isoleucine residue. The possible effects of this point mutation were predicted by multiple algorithms which showed no alteration of the secondary structural arrangement at or in the proximity of the mutated residue, the disorder propensity predicted for the mutant were highly similar to those obtained for the wild-type. In agreement with this, the sequence-based prediction of stability changes also implied neutral nature of the mutation (-0.37 kcal/mol). We predicted no significant increase or decrease of free energy change value upon p.(Thr992Ile) mutation. Similar to RB protein, no local or global disturbances of the structure could be predicted, rather functional changes of the residue in 992th position may be responsible for the phenotypic effects.

Interaction analysis between RB and MET protein

Based on data available in BioGRID and STRING databases, no direct interaction between RB1 and MET proteins could be established. This is supported by the different subcellular localizations of the wild-type proteins, as RB1 and MET act in diverse subcellular compartments (in the nucleoplasm and in the cytoplasm, respectively).

However, RB1 and MET share multiple interaction partners. Based on BioGRID database, common interacting partners include CDK4, CDK6, GRB2, MYC, and RAF1 proteins, as well. Thus, simultaneous functional changes of RB1 and MET may basically transactivate the existing signaling networks.

Discussion

The c.2548C>T; p.(Gln850Ter) *RB1* germline gene variant is registered in the COSMIC databases, but no relation to Rb was documented so far. Therefore, this was the first time to describe the variant in Rb. Germline loss of function *RB1* gene mutations are known to be causative in Rb [6] and are associated with increased risk of osteosarcoma development [20]. The predisposition to sarcomas has been attributed to genetic susceptibility due to inactivation of the *RB1* gene as well as to the genotoxic effect of radiotherapy applied to treat Rb. Bone and soft tissue sarcomas in hereditary Rb survivors occur most frequently within the radiation field in the facial bone (orbita), but they may also occur elsewhere.*RB1* alterations also serve as unfavourable prognostic marker for the clinical classification and management of osteosarcoma patients [21].

In agreement with RB protein disordered structure, the C-terminal region has already been reported to enable protein-protein interactions. Structural studies revealed interactions of RB protein with heterodimer of E2F transcription factor 1 (E2F1) and transcription factor Dp-1 (DP1 (829-874) [18], with catalytic subunit of protein phosphatase 1 (PP1c) (870-882) [19], with complex of cyclin dependent protein kinase 2 (CDK2) and cyclin A (868-878) [20], and with mouse importin-α (858-877) [19] (numbers in parentheses show regions of retinoblastoma-associated protein that form interactions in the complexes) (**Figure 3**).

Additionally, interactions between the RB protein and the complex of cyclin dependent protein kinase 9 (CDK9) and cyclin T2 were also reported and this mutagenesis study revealed that the interactions were mediated by the C-terminus of RB protein (835-928) [22]. Out of these proteins only E2F1 has exclusive nuclear localization based on Human Protein Atlas [23], the other relevant human proteins are localized in the cytoplasm. Consequently, deletion of the region 851-928 of RB protein most probably influences a series of functionally relevant protein-protein interactions, rather, than deletion-induced structural changes promoting directly the pathogenic phenotype.

The diversity of cancers in which *MET* mutations have been identified suggests that mutationally actived MET protein plays a significant role in the tumorigenic process in a wide range of cell types. The juxtamembran domain mutations were shown to attenuate MET receptor ubiquitination and degradation and prolong MET signaling [24]. There are no eukaryotic linear motifs in MET protein which include Thr1010 residues, but based on PhosphoSitePlus database [25] this residue is known to be phosphorylated. The functional characteristics of p.(Thr1010Ile) sequence variant has already been reported. However, transforming nature of this variant was described in a study. The investigation revealed that this variant was present in individuals with or without cancer, and no evidence was found regarding the transformative capacity of p.(Thr1010Ile) variant [26]. This finding may indicate that the structural integrity of MET is retained in the mutant. However, structural consequences of the p.(Thr1010Ile) variant were not investigated so far. In the COSMIC database, this mutation was described as gemline and somatic form as well. It proved to be more active than the wild-type MET in the athymic nude mice tumorigenesis assay, suggesting its potential effect on tumorigenesis [27].

In a novel large cohort study, patients with heritable Rb had a significantly increased risk for second tumor, while patients with nonheritable Rb did not. The overall mortality rate was 48% for heritable Rb and 23% for patients with nonheritable form. The cumulative mortality rate from second cancers at the age 60 years was 34% among those with heritable Rb and 12% among those with nonheritable Rb. Sarcoma was the most common histological type of malignancy in patients with heritable Rb, and carcinoma was the most common type in nonheritable Rb [28].

Loss of *RB1* gene function has also been found to be associated with increased risk of osteosarcoma metastasis and a poor histological response to chemotherapy, compared with osteosarcoma patients with intact *RB1* fuction [29]. The response of osteosarcoma patients to chemotherapy was assessed by the degree of histological necrosis of tumor tissues induced by chemotherapy. The majority of bone sarcomas occured within the radiation field in the head region, but up to 40% were diagnosed outside the treatment field, primarily in the lower extremities. Osteosarcoma is most frequently seen in the femur and osteoblastic osteosarcoma is the most common histological subtype making up 41-89% of this malignancy [21]. But both chondrosarcoma and Ewing sarcoma have been reported [30]. Sarcomas occuring in the radiation field were diagnosed with a lag time one year shorter than those diagnosed outside of the field [5]. This timing suggests that diverse biologic mechanism may be involved with bone sarcoma development including radiation damage and anatomical site. In our study, we demonstrated different somatic mutation profiles for sarcomas with chondroblastic and osteoblastic phenotypes by the use of a 67 gene solid tumor NGS panel. *TP53* and other gene aberrations were limited to the osteoblastic form of the lower extremity, suggesting an independent evolution from the chondroblastic type originating at the site of the irradiation therapy.

The loss or inactivation of *RB1* function results in a significant 1.62-fold increase in the mortality rates in patients with osteosarcoma compared with those in patients without this gene aberratios [21]. Osteosarcoma is characterised by its high potential to metastise to the lungs or other bones [31]. Mutations of the *RB1* gene result in its dissociation from E2F and subsequent transcription of multiple genes involved in cell cycle progression lead to malignant transformation and the progression of osteosarcoma [32]. Metastatic osteosarcoma is typically difficult to control and known to indicate poor prognosis [33].

Because of the expanding number of registered Rb cases [28], the novel rare cases publication is very important to understand the molecular mechanism of this malignancy. To the best of our knowledge, this is the first report to detect this novel form of *RB1* mutation and synchronous *MET* gene mutation causing

6

non-heritable bilateral retinoblastoma and consequential chondroblastic and osteoblastic osteosarcoma, the latter one developing pulmonary metastatses. Structural and functional prediction of the germline mutant proteins suggested an indirect parallel involvement in the pathogenesis of this uniqe series of retinoblastoma related neoplasias. The results of the 67 gene NGS panel clearly differentiated the histologically identified osteosarcoma types by two different sets of gene variants.

Conflicts of Interest:

The authors declare that they have no potential conflicts of interest to disclose.

Author contributions:

A.M.: methodology, writing, draft preparation and supervision; J.M.: protein analysis, draft preparation; E.S.B., P.J., Y.C.C.: histology, autopsy; L.M.: clinical genetic methology and supervision; I.Sz., C.K.: clinical contributions, follow up, and writing; G.M.: conceptualization, writing, and supervision.

All authors have read and agreed to the submitted version of the manuscript.

References

1. Kivelä T. The epidemiological challenge of the most frequent eye cancer: retinoblastoma, an issue of birth and death. Br J Ophthalmol , 2009 93: 1129–1131.

2. Zajaczek S, Jakubowska A, Kurzawski G, Krzystolik Z, Lubiński J. Age at diagnosis to discriminate those patients for whom constitutional DNA sequencing is appropriate in sporadic unilateral retinoblastoma. Eur J Cancer Oxf Engl 1990 , 1998 34: 1919–1921.

3. Dimaras H. Retinoblastoma genetics in India: From research to implementation. Indian J Ophthalmol , 2015 63: 219–226.

4. Guérin S, Hawkins M, Shamsaldin A, Guibout C, Diallo I, Oberlin O, Brugières L, de Vathaire F. Treatment-adjusted predisposition to second malignant neoplasms after a solid cancer in childhood: a case-control study. J Clin Oncol Off J Am Soc Clin Oncol , 2007 25: 2833–2839.

5. Chauveinc L, Mosseri V, Quintana E, Desjardins L, Schlienger P, Doz F, Dutrillaux B. Osteosarcoma following retinoblastoma: age at onset and latency period. Ophthalmic Genet , 2001 22: 77–88.

6. Singh J, Mishra A, Pandian AJ, Mallipatna AC, Khetan V, Sripriya S, Kapoor S, Agarwal S, Sankaran S, Katragadda S, Veeramachaneni V, Hariharan R, Subramanian K, Mannan AU. Next-generation sequencing-based method shows increased mutation detection sensitivity in an Indian retinoblastoma cohort. Mol Vis , 2016 22: 1036–1047.

7. Akdeniz D, Tuncer SB, Kebudi R, Celik B, Kuru G, Kilic S, Sukruoglu Erdogan O, Avsar M, Buyukkapu Bay S, Tuncer S, Yazici H. Investigation of new candidate genes in retinoblastoma using the TruSight One "clinical exome" gene panel. Mol Genet Genomic Med, 2019 7: e785.

8. Garnier J, Gibrat JF, Robson B. GOR method for predicting protein secondary structure from amino acid sequence. Methods Enzymol , 1996 266: 540–553.

9. Mészáros B, Erdos G, Dosztányi Z. IUPred2A: context-dependent prediction of protein disorder as a function of redox state and protein binding. Nucleic Acids Res , 2018 46: W329–W337.

10. Kumar M, Gouw M, Michael S, Sámano-Sánchez H, Pancsa R, Glavina J, Diakogianni A, Valverde JA, Bukirova D, Čalyševa J, Palopoli N, Davey NE, Chemes LB, Gibson TJ. ELM-the eukaryotic linear motif resource in 2020. Nucleic Acids Res , 2020 48: D296–D306.

11. Capriotti E, Fariselli P, Casadio R. I-Mutant2.0: predicting stability changes upon mutation from the protein sequence or structure. Nucleic Acids Res , 2005 33: W306-310.

12. Stark C, Breitkreutz B-J, Reguly T, Boucher L, Breitkreutz A, Tyers M. BioGRID: a general repository for interaction datasets. Nucleic Acids Res , 2006 34: D535-539.

13. Szklarczyk D, Gable AL, Lyon D, Junge A, Wyder S, Huerta-Cepas J, Simonovic M, Doncheva NT, Morris JH, Bork P, Jensen LJ, Mering C von. STRING v11: protein-protein association networks with increased coverage, supporting functional discovery in genome-wide experimental datasets. Nucleic Acids Res , 2019 47: D607–D613.

14. Hassler M, Singh S, Yue WW, Luczynski M, Lakbir R, Sanchez-Sanchez F, Bader T, Pearl LH, Mittnacht S. Crystal structure of the retinoblastoma protein N domain provides insight into tumor suppression, ligand interaction, and holoprotein architecture. Mol Cell , 2007 28: 371–385.

15. Burke JR, Hura GL, Rubin SM. Structures of inactive retinoblastoma protein reveal multiple mechanisms for cell cycle control. Genes Dev , 2012 26: 1156–1166.

16. Rubin SM, Gall A-L, Zheng N, Pavletich NP. Structure of the Rb C-terminal domain bound to E2F1-DP1: a mechanism for phosphorylation-induced E2F release. Cell , 2005 123: 1093–1106.

17. Hirschi A, Cecchini M, Steinhardt RC, Schamber MR, Dick FA, Rubin SM. An overlapping kinase and phosphatase docking site regulates activity of the retinoblastoma protein. Nat Struct Mol Biol , 2010 17: 1051–1057.

18. Lowe ED, Tews I, Cheng KY, Brown NR, Gul S, Noble MEM, Gamblin SJ, Johnson LN. Specificity determinants of recruitment peptides bound to phospho-CDK2/cyclin A. Biochemistry , 2002 41: 15625–15634.

19. Fontes MRM, Teh T, Jans D, Brinkworth RI, Kobe B. Structural basis for the specificity of bipartite nuclear localization sequence binding by importin-alpha. J Biol Chem , 2003 278: 27981–27987.

20. Kleinerman RA, Schonfeld SJ, Tucker MA. Sarcomas in hereditary retinoblastoma. Clin Sarcoma Res , 2012 2: 15.

21. Ren W, Gu G. Prognostic implications of RB1 tumour suppressor gene alterations in the clinical outcome of human osteosarcoma: a meta-analysis. Eur J Cancer Care (Engl) , 2017 26.

22. Simone C, Bagella L, Bellan C, Giordano A. Physical interaction between pRb and cdk9/cyclinT2 complex. Oncogene , 2002 21: 4158–4165.

23. Pontén F, Jirström K, Uhlen M. The Human Protein Atlas–a tool for pathology. J Pathol , 2008 216: 387–393.

24. Tovar EA, Graveel CR. MET in human cancer: germline and somatic mutations. Ann Transl Med , 2017 5: 205.

25. Hornbeck PV, Zhang B, Murray B, Kornhauser JM, Latham V, Skrzypek E. PhosphoSitePlus, 2014: mutations, PTMs and recalibrations. Nucleic Acids Res , 2015 43: D512-520.

26. Tyner JW, Fletcher LB, Wang EQ, Yang WF, Rutenberg-Schoenberg ML, Beadling C, Mori M, Heinrich MC, Deininger MW, Druker BJ, Loriaux MM. MET receptor sequence variants R970C and T992I lack transforming capacity. Cancer Res , 2010 70: 6233–6237.

27. Lee JH, Han SU, Cho H, Jennings B, Gerrard B, Dean M, Schmidt L, Zbar B, Vande Woude GF. A novel germ line juxtamembrane Met mutation in human gastric cancer. Oncogene , 2000 19: 4947–4953.

28. Gregersen PA, Olsen MH, Urbak SF, Funding M, Dalton SO, Overgaard J, Alsner J. Incidence and Mortality of Second Primary Cancers in Danish Patients With Retinoblastoma, 1943-2013. JAMA Netw Open , 2020 3: e2022126.
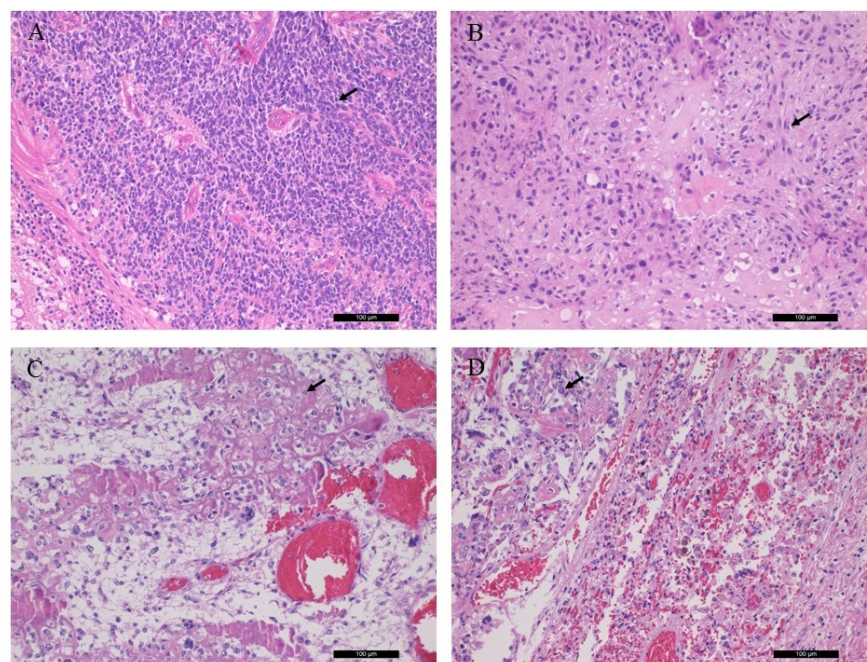
8

29. Benassi MS, Molendini L, Gamberi G, Sollazzo MR, Ragazzini P, Merli M, Magagnoli G, Sangiorgi L, Bacchini P, Bertoni F, Picci P. Altered G1 phase regulation in osteosarcoma. Int J Cancer , 1997 74: 518–522.

30. Moll AC, Imhof SM, Schouten-Van Meeteren AY, Kuik DJ, Hofman P, Boers M. Second primary tumors in hereditary retinoblastoma: a register-based study, 1945-1997: is there an age effect on radiation-related risk? Ophthalmology , 2001 108: 1109–1114.

31. Ritter J, Bielack SS. Osteosarcoma. Ann Oncol Off J Eur Soc Med Oncol , 2010 21 Suppl 7: vii320-325.

32. Henley SA, Dick FA. The retinoblastoma family of proteins and their regulatory functions in the mammalian cell division cycle. Cell Div , 2012 7: 10.

33. Herzog CE. Overview of sarcomas in the adolescent and young adult population. J Pediatr Hematol Oncol , 2005 27: 215–218.
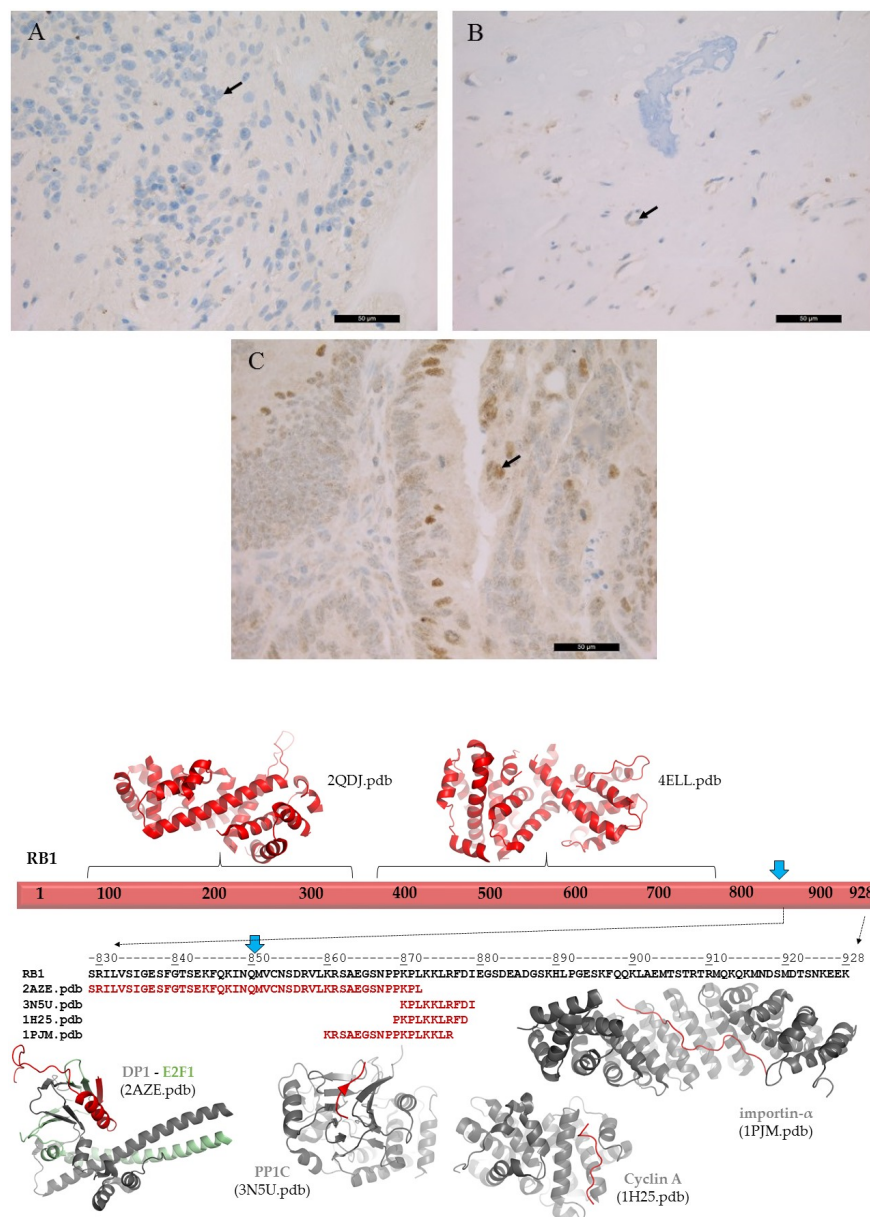
Figure legend

Figure 1. Conventional histological (H&E) characteristics of patient tumor samples. **A** : Rb of the right eye bulb, **B** : chondroblastic osteosarcoma of the left orbital bone, **C** : osteoblastic osteosarcoma from the left tibia, **D** : osteoblastic osteosarcoma, pulmonary metastasis. Arrows indicate retinoblasts, as well as chondroblastic and osteoblastic propagation (magnification: x20).

Figure 2. Immunohistochemistry of RB protein. **A** : retinoblastoma (S1), **B** : left orbital bone (S3), **C** : colorectal adenocarcinoma control. Arrows indicate the IHC-negative cell nuclei of retinoblastic/ chondroblastic tumors and the positive nuclear staining in adenocarcinoma cells (magnification: x40).

Figure 3. Structure and interactions of RB1. Schematic represenation of full-length RB1 protein is shown. The structures of N-terminal and central regions are represented, and the protein-protein interactions of C-terminal region are also shown based on structural data. Sequence of the C-terminal of region of RB1 is shown by black color. Blue arrows show position of p.Gln850Ter mutation. The sequences that are involved in protein-protein interactions are shown for each coordinate file, these regions are highlighted by red in the complex structures, as well.

Hosted file

Table 1.pdf available at https://authorea.com/users/374740/articles/492196-novel-germline-rb1-and-met-gene-mutations-in-a-case-with-bilateral-retinoblastoma-followed-by-multiple-metastatic-osteosarcoma

Hosted file

Table 2.pdf available at https://authorea.com/users/374740/articles/492196-novel-germline-rb1-and-met-gene-mutations-in-a-case-with-bilateral-retinoblastoma-followed-by-multiple-metastatic-osteosarcoma